

1 **An approach to the modelling of stability of waste containers during urban flooding**

2 Eduardo Martínez-Gomariz^{a,e*}, Beniamino Russo^{b,c}, Manuel Gómez^{a,e}, Aurea Plumed^d

3 ^a*CETaqua Water Technology Centre, Barcelona, Spain*

4 ^b*AQUATEC (SUEZ Advanced Solutions), Barcelona, Spain*

5 ^c*Group of Hydraulic and Environmental Engineering, Technical College of La Almunia (EUPLA),*
6 *University of Zaragoza, Spain*

7 ^e*Flumen Research Institute, Civil and Environmental Engineering Department, Technical University of*
8 *Catalonia, Spain*

9 ^d*Barcelona City Council, Operational Management Department, Cleaning and Waste Management*
10 *Facilities Direction, Barcelona, Spain*

11 *Corresponding author. Email: eduardo.martinez@cetaqua.com

12 **Abstract:** Before the solid waste is dumped in landfills, the collection process for
13 large Spanish cities starts from a regular collection of household waste municipal
14 service which is carried out through street containers. When an urban flood occurs
15 those containers may lose their stability, thereby allowing debris (i.e. solid waste
16 contained) and leachate to escape from the container and contaminate the flood
17 water. Moreover, once a container loses its stability it can further constrict a narrow
18 street and increase flooding, thereby creating a closed basin with no outlet for
19 runoff and exacerbating the effects of flooding. Therefore, the waste containers
20 stability when exposed to flooding is definitely an environmental, safety and health
21 concern to be addressed. In this research stability functions for waste containers
22 exposed to urban floods have been derived. These thresholds have been employed
23 to analyse the containers' potential behaviour during floods in Barcelona. In order
24 to validate the model a historical rainfall has been modelled and low-return-period
25 design storms (i.e. 2, 5 and 10 years) have been used to assess the containers
26 vulnerability against floods for frequent rainfall events. Once the number of
27 potentially unstable containers has been estimated, an adaptation measure has been
28 proposed in order to increase the resilience of waste sector against urban floods in
29 Barcelona.

30 **Keywords:** Waste containers; urban floods; environment; safety; health.

31 **1. Introduction**

32 Cities around the world, can be affected by floods. However, urban floods may have different
33 sources and are called riverine flood, when the main river bed exceeds its capacity; stormwater
34 flood, when the conveyance capacity of the urban drainage system is exceeded; or coastal flood,
35 when the seawater causes the flooding. Only stormwater floods may affect any city, even if
36 neither is a coastal city nor have a nearby river to be overflowed (Zbigniew W. *et al.*, 2014; Patra
37 *et al.*, 2016).

38 Stormwater flooding occurs because the “exceedance flow” is generated on the urban
39 surface. For this reason, the design of drainage systems should consider the dual drainage concept
40 (Djordjevic *et al.*, 1999; Schmitt *et al.*, 2004; Nanía *et al.*, 2015; Russo *et al.* 2015), through which
41 certain amount of runoff is assumed to flow on the streets because only a portion of runoff can be
42 conveyed by the sewer system. The term pluvial flooding is sometimes used synonymously with
43 stormwater flooding, or sometimes used to denote urban flooding where there is no sewer network
44 or the network is already at full capacity (Butler and Davies, 2011). When accepting the dual
45 drainage concept, the consequences of this flow on the streets must be analysed by ensuring firstly
46 a high level of safety for pedestrians (Martínez-Gomariz *et al.* 2016) but also minimizing the
47 direct and indirect economic damages. Therefore, a comprehensive flood risk assessment must be
48 conducted in order to implement adaptation measures if necessary.

49 On the other hand, the action of protecting against and planning responses to a wide range
50 of security challenges that threaten cities and urban areas (i.e. from flooding to terrorism) has
51 been referred to as “urban resilience”. Therefore, according to Coaffee *et al.* (2008), urban
52 resilience refers to both the design alterations and managerial and governance measures that seek
53 to prevent or mitigate the physical and social vulnerability of areas (i.e. protecting life, properties
54 and economic activities).

55 Even though, a wide range of urban resilience definitions can be found within the research
56 literature, some authors addressing this concern (Meerow *et al.*, 2016) state that the common
57 definition should balance the need to clarify theoretical inconsistencies while retaining requisite

58 flexibility. Moreover, applying resilience in different contexts requires answering: Resilience for
59 whom and to what? When? Where? And why? (Meerow *et al.*, 2016). According to these
60 resilience definitions, when dealing with and proposing adaptation measures for urban floods we
61 are, in fact, acting to improve the urban resilience to flooding or urban flood resilience.

62 Adaptation measures to improve urban flood resilience span a range of technical subject
63 areas which, apart from hydrological and hydraulic flood studies, should include urban planning
64 and design, urban drainage, building construction and asset management of infrastructure
65 networks (Escarameia 2016). Furthermore, it should be borne in mind that an urban area has to
66 be considered as an entity composed by different elements and not merely as a set of buildings
67 (Lhomme *et al.*, 2013). It is acknowledged that it is an interesting and useful exercise to think of
68 a city as a system (Zevenbergen *et al.*, 2010). This system is formed by different sectors (i.e.
69 water, power, mobility, waste and telecommunications), which, in turn, are comprised of several
70 urban services and infrastructures.

71 The EU funded RESCCUE project (RESilience to cope with Climate Change in Urban
72 arEas; www.resccue.eu), in which this study is framed, aims at helping cities to become more
73 resilient to physical, but also social and economic challenges by generating models and tools to
74 bring this objective to practice. In a comprehensive urban resilience assessment within RESCCUE
75 project, interdependencies and cascading effects due to failure caused by climate event impacts
76 are taken into account. This assessment is carried out through two different scales approaches: a
77 holistic study (an all-city study by employing the Hazur® platform) (Evans *et al.*, 2018), and
78 specific studies for different urban services affected by a specific climate event, such as municipal
79 solid waste management affected by floods.

80 Municipal solid waste management and wastewater contribute about 3 per cent to current
81 global anthropogenic greenhouse gas emissions, about half of which is methane from landfills.
82 One forecast suggests that without mitigation, this could double by 2020 and quadruple by 2050
83 (UN-HABITAT, 2010). For this reason, most research studies are focused on studying mitigation
84 strategies to deal with greenhouse gas emissions due to landfills. Mitigation needs to be a mix of

85 the ‘technical fix’ approach, such as landfill gas collection and utilization, and upstream measures,
86 particularly reduction, reuse, recycling and composting. Solid waste management, often a
87 neglected aspect of urban management, is a problem in both developed and developing countries
88 (Sam, 2002) and there are reasons (Lamond *et al.*, 2012) to consider serious issues in flood risk
89 management: a) blockages in drainage and watercourses because of a poor disposal of waste,
90 which reduces their conveyance and leads to flooding; b) debris in floodwaters can cause
91 increased damage to property and increase the economic impacts; c) deposition of waste, after a
92 flood, can block access and be a source of toxins and breeding ground for disease; and d) leaching
93 of toxins into groundwater.

94 Only a few studies focused on the impacts caused by climate change on waste sector
95 (Zimmerman *et al.*, 2010; Winne *et al.*, 2012; USAID, 2012, 2014, 2015). By assuming more
96 intense rainfall events, potential impacts on solid waste management are described, such as:
97 saturated soils and decreased stability of slopes and landfill linings at waste management sites;
98 increased risk of flooding (fluvial and flash floods) affecting facilities, access and use of mobile
99 plant; increased risk of flood-related disruption to critical infrastructure and suppliers (transport,
100 energy, ICT, etc.).

101 As stated, the main research effort regarding climate change-related impacts of solid
102 waste sector is focused on offering mitigation measures and strategies in order to reduce the waste
103 greenhouse gases emissions. However, no research studies addressed the reverse problem: how
104 climate change impacts on solid waste sector. Landfills are mainly in the centre of these studies,
105 offering adaptation measures in order to increase the resilience of this sector when impacted by
106 different hazards resulting from climate change (e.g. more frequent urban floods). Nevertheless,
107 before the solid waste is dumped in landfills, the collection process for large Spanish cities starts
108 from a regular collection of household waste municipal service which is carried out through street
109 containers. Therefore, when an urban flood occurs those containers may lose their stability,
110 thereby allowing debris (i.e. solid waste contained) and leachate to escape from the container and
111 contaminate the flood water. Also the container itself may be washed away (i.e. a massive debris)

112 together or separately with its content (Figure 1). Such type of massive debris carried by
113 floodwaters, similar to vehicles (Martínez-Gomariz *et al.*, 2018), can further constrict a narrow
114 street and increase flooding, thereby creating a closed basin with no outlet for runoff and
115 exacerbating the effects of flooding. This hazard is greatest upstream of culverts, bridges, or other
116 places where debris can collect. On the other hand, inlets and sewers can become clogged with
117 solid waste if it comes out of the container after it loses stability, thereby worsening the drainage
118 system and contributing to exacerbate the flood impacts. Consequently, the waste containers
119 stability when exposed to flooding is definitely an environmental, safety and health concern to be
120 addressed.

121 The main cascading effects due to containers' instabilities may be listed as follows:

- 122 • **Traffic disruption:** Traffic may be disrupted not just while flood is occurring
123 but also after the event when these containers that were washed away may be left
124 on roads.
- 125 • **Waste collection disruption:** After a flood event, the waste collection may be
126 disrupted if containers were moved from their original location. The municipal
127 workers have to relocate them and even collect their content in case it came out
128 from the container after losing the stability.
- 129 • **Potential sewer blockages:** Potential fractions coming out from the container
130 may block sewers and thereby adversely affect the drainage efficiency.
- 131 • **Increased likelihood of cascading effects due to flooding:** If containers, moved
132 from their original position, lay at narrow streets or accumulate at inlets, culverts
133 or bridges, water depths may increase and therefore the flood consequences will
134 be aggravated. A flood without important consequences may turn into a flood
135 which cause a cascading effect to other sectors.

136 The present research focuses on the stability of the containers when exposed to urban
137 floods that Barcelona City Council has distributed across the city to provide waste collection to
138 citizens. A description of how waste and recycling collection is managed in Barcelona together

139 with the description of the types of containers and which kind of fractions they may contain is
140 presented first. Afterwards, a comprehensive study of the forces acting on a flooded container,
141 the different modes of instabilities and the derivation of the formula for the stability threshold
142 (i.e. the velocity and water depth combinations which lead to the containers instability) is
143 conducted. Finally, these obtained stability thresholds are employed to analyse the potential
144 behaviour of containers against floods in Barcelona caused by historical and low-return-period
145 design storms (i.e. 2, 5 and 10 years). Adaptation measures in order to improve the resilience of
146 waste sector against urban floods in Barcelona will be proposed based on the results of the case
147 study of the stability of containers exposed to flooding.

148 **2. Waste and recycling collection service by containers in** 149 **Barcelona**

150 ***2.1. Description of waste and recycling Barcelona municipal service***

151 Barcelona has an extensive municipal service for a daily collection of household and commercial
152 waste to provide waste collection to citizens and ensure a clean and healthy public space. This
153 service is carried out through street containers, door to door bags collection service, pneumatic
154 collection boxes and bins for collection in shops. Waste which cannot be placed in conventional
155 containers is delivered to Green Dots. Citizens also have special services regarding waste
156 collection, such as old furniture and clothes, dead animals, debris bags gardening waste,
157 fibrocement or asbestos.

158 Taking part in the recycling waste collection is the first step in dividing household waste
159 and a civic gesture which contributes to preserving the environment. Waste can be reused by
160 recycling it, so it can become a resource and provide environmental and social benefits for
161 everyone. In the context of public awareness campaigns, Barcelona City Council is promoting
162 actions and tools to accompany the citizens in improving household waste collection through
163 educational activities and training which are addressed at the public and groups from the city.

164 Barcelona opts for a recycling collection including five different fraction-types of
165 containers. There are containers for each one of them located citywide in order to make waste
166 management easier: waste, organic, paper and cardboard, packaging, and glass. All citizens have
167 recycling collection containers located less than 100 meters from their home.

168 ***2.2. Type of containers and fractions characterization***

169 In Barcelona there are a total of 27,134 containers, which can be classified either according to the
170 fraction they contain (i.e. waste, organic, paper and cardboard, packaging, and glass), their
171 volume in litres (i.e. 3,200; 3,000; 2,400; 2,200; and 1,800) or the way they are loaded (i.e. lateral,
172 bilateral, rear, underground). The percentage distribution according to their fractions is as follows:
173 44% (waste), 22% (organic), 12% (paper and cardboard), 11% (packaging), and 11% (glass).
174 Regarding their loading their distribution is as follows: 62% (lateral), 25% (bilateral), 12% (rear),
175 and 1% (underground).

176 Due to the less percentage of rear and underground loading-type containers when
177 comparing with lateral and bilateral type (Figure 2), only the former have been taken into
178 account in this study, which is an 87% of the total number of containers. Table 1 and Figure 3
179 show the distribution of studied containers both per districts and type of fraction.

180 The positioning of the containers in the city is as follows: these are placed in groups of
181 4 or 5, one per type of fraction to be collected, and their position on the streets is established
182 either by painting enclosed areas on the ground or by defining their area with plastic yellow
183 pieces, which are used also as guides to place the containers on it (Figure 4). That is the reason
184 for the containers to have a hollow along their base, to place the yellow guides on it. These
185 hollows, as will be explained later, contribute to a better stability against the buoyancy.
186 In order to analyse the containers stability, an important parameter is their weight, which can vary
187 greatly depending on their filling degree and the type of contained fraction. Moreover, when it
188 comes to different fractions inside the containers the concept of bulk density has to be presented.
189 In contrast to density, bulk density is only used in cases where the particles or chunks of matter

190 are loosely packed with space for air within. Therefore, bulk density is not an intrinsic property
191 of a material, in contrast to density (DifferenceBetween.com, 2011). The following bulk densities
192 (kg/m^3) for the different fractions have been proposed, based on the values recommended by the
193 Cogersa-AstUR project (n.d.) and The Spanish Ministry of Agriculture and Fisheries, Food and
194 Environment (MAPAMA, n.d.): a) Waste (113.92); b) Organic (387.5); c) Paper and cardboard
195 (70); d) Glass (330); and e) Packaging (26.5).

196 Therefore, the container weight can be defined as a linear function depending on the
197 type of fraction (i.e. the slope of the function) and the filling percentage (1).

$$W(m_i, p) = W_o + m_i \cdot p / 100 \quad (1)$$

198 where $W(\text{kg})$ is the container total weight, $W_o(\text{kg})$ is the unladen container weight, $m_i(\text{kg})$ is
199 the slope of the function related to each type of fraction, and $p(\%)$ is the percentage value of the
200 filling.

201 Figure 5 plots, as example, the weight linear functions for a 3,200l lateral container for the three
202 types of fraction that this container might contain.

203 In Table 2, all basic characteristics for the considered containers in this study are
204 collected, grouped according to the type of loading, volume and fractions. The considered
205 important parameters are: Ground Clearance (GC) (i.e. the distance from the ground to the body
206 of the container), width and depth (L1 and L2 respectively), volumes of hollows at the base of
207 each type of container (V_{hollow1} and V_{hollow2}), unladen weight, and the slope of the weight linear
208 function related to each fraction and container volume (see Figures 7, 8 and 9).

209 **3. Containers stability when exposed to flooding**

210 ***3.1. Forces and torques acting on a flooded container***

211 Two types of forces and torques may be considered in order to analyse the stability of such urban
212 elements exposed to flooding, those due to the water flow (i.e. hydrodynamic forces) and those
213 due to the container contact with the ground (Figure 6). Focusing firstly on hydrodynamic forces,

214 drag force (F_D) and vertical pushing force (F_v) are the ones that may affect the container stability.

215 Drag force (F_D) may be expressed as follows:

$$F_D = \frac{1}{2} \rho_w v^2 C_d A \quad (2)$$

216 where ρ_w is the water density, v is the water velocity, C_d is the drag coefficient, which depends
217 on Reynolds number and the shape of the container (i.e. rectangular prism), and A is the projected
218 area of the submerged container part perpendicular to the flow direction. The other hydrodynamic
219 force is the vertical pushing force (F_v) which is the combination of the lift force (F_L) and the
220 buoyancy force (F_b) (Martínez-Gomariz *et al.*, 2017). A container is expected to lose its stability
221 for low or zero (i.e. hydrostatic conditions) once the water depth reaches the buoyancy depth,
222 therefore, for simplicity, only buoyancy force, even for hydrodynamic conditions, is considered
223 in this study ($F_v \approx F_b$).

224 According to Archimedes' principle, the buoyancy force acting on a flooded container is
225 defined as expression (3) indicates.

$$F_b = V_{disp} \cdot \gamma_w \quad \text{assuming } V_{disp} \approx L_1 \cdot L_2 \cdot y \quad (3)$$

226 Where V_{disp} is the displaced container volume, L_1 and L_2 are the container width and
227 depth respectively, γ_w is the specific weight of water, and y is the water depth.

228 Nevertheless, the container is expected to become buoyant for low water depths, thus the
229 contribution of the containers bottom hollows on reducing buoyancy will likely be significant.
230 For this reason, these hollows (Figure 8) have been considered by deriving a function ($V_h(y)$)
231 (Figure 9) to determine the water-filled hollows volume (V_{h1} (lateral and bilateral) and V_{h2}
232 (lateral)) for both types of containers (i.e. lateral and bilateral loading). This volume will be taken
233 off the one assumed as completely solid (3); consequently, the displaced volume will be obtained
234 based on the expression (4). Once the water depth reaches the hollows depths (y_{hi}), this volume
235 (V_{himax}) remains constant (Figure 9).

$$V_{disp} \approx (L_1 \cdot L_2 \cdot y) - V_h(y) \quad (4)$$

236 On the other hand, gravitational and frictional forces will act as stabilizing forces in this
237 system of forces. The first, gravitational force (F_g), depends on the container weight ($W(m_i, p)$),
238 which in turn depends on their unladed weight (W_o), the container filling (p), and the type of
239 fraction that it contains (m_i) as described in section 2.2. Accordingly, gravitational force can be
240 obtained as indicated in expression (5).

$$F_g = W(m_i, p) \cdot g = (W_o + m_i \cdot p / 100) \cdot g \quad (5)$$

241 where g (m/s^2) is the gravitational acceleration.

242 However, the gravitational force stabilization will be countered by the vertical pushing
243 force action, to some extent, depending on the water depth. Therefore, the so-called effective
244 weight (F_G) may join the action of both forces ($F_G = F_g - F_v$), so that the resulting F_G will
245 determine the vertical force stabilization.

246 Previous statements only are true in case the container is located on a flat ground, thereby
247 considering only vertical component for the normal ground reaction (F_N). Consequently, the
248 frictional force (F_R) may be obtained according to the expression (6).

$$F_R = \mu \cdot (W \cdot g) = \mu \cdot (W_o + m_i \cdot p) \cdot g \quad (6)$$

249 where μ is the friction coefficient between container and ground.

250 **3.2. Modes of instabilities**

251 Different modes of instability may occur when a container is flooded (Figure 10). In case
252 of stagnant water only buoyancy may act on the flooded container, and it will occur when the
253 buoyancy force reaches the gravitational one. On the other hand, hydrodynamic instabilities may
254 occur also, by either combining effects or acting isolated. Sliding instabilities will occur when the
255 drag force exceeds the frictional one, and toppling will take place in case of container rotation
256 from one corner of its base. In reality, both instabilities will likely occur together, when after
257 sliding the container may be blocked by an object located on the ground and is toppled. The

258 yellow guides placed on the ground (Figure 4) to define the container placing area and also to fix
 259 the location of the containers themselves, could be a reason for container toppling. Regarding this
 260 yellow plastic pieces, it has to be considered that could be supportive in terms of stability in
 261 certain situations. However, the less favourable conditions have been taken into account in this
 262 study, thus the guides effect has been neglected herein.

263 3.2.1. Buoyancy

264 Critical or buoyant water depth can be obtained by establishing the equilibrium condition
 265 for buoyancy (7). It can be seen also as the water depth for which the previously defined container
 266 effective weight (F_G) becomes zero.

$$F_b = F_g \quad (7)$$

267 Based on this equilibrium condition, and on the buoyancy force expression (8), a critical
 268 or buoyant water depth may be derived (9).

$$F_b = [(L_1 \cdot L_2 \cdot y) - V_h(y)] \cdot \gamma_w \quad (8)$$

$$y_b = \frac{(W_o + m_i \cdot p) \cdot g + V_h(y) \cdot \gamma_w}{L_1 \cdot L_2 \cdot \gamma_w} + GC \quad (9)$$

269 By applying expression (8), all critical water depths, for the different types of container
 270 with their respective characteristics (Table 2), have been calculated according to Table 3. Since
 271 the container weight depends on its filling, three filling scenarios have been taken into account:
 272 empty, half-full, and completely full.

273 A great variety of buoyancy depths has been obtained, ranging from 0.106 m (lateral
 274 loading, 3,200 litres, empty, and packaging fraction) to 0.640 m (lateral loading, 2,200 litres, full,
 275 and organic fraction).

276 3.2.2. *Sliding and toppling instability*

277 Although the critical water depth in terms of buoyancy (i.e. hydrostatic conditions) has
278 been obtained (Table 3), the container stability may be compromised for lower water depths when
279 the flow velocity (i.e. hydrodynamic conditions) comes into play. As described previously,
280 sliding, toppling or even both if it topples after being slid away, are the modes of containers
281 instability which can arise, apart from buoyancy mode. Therefore, in this section the critical
282 velocity functions are derived for both modes, sliding and toppling, based on establishing
283 equilibrium condition for both modes as expressions (10), (11), (12) and (13) indicate, and
284 according to the system of forces depicted on Figure 6.

285 **Equilibrium condition for sliding**

$$\sum F_H = 0 \quad (10)$$

$$F_D = F_R \rightarrow \frac{1}{2} \rho_w v^2 C_d A = \mu F_G = \mu (F_g - F_v) \quad (11)$$

286 where F_H are the different horizontal forces acting on the flooded container.

287 **Equilibrium condition for toppling**

$$\sum M_0 = 0 \quad (12)$$

$$M_{F_D} = M_{F_G} \rightarrow F_D \cdot \frac{1}{2} y = F_G \frac{1}{2} L_2 \quad (13)$$

288 where M_0 are the torques produced on the flooded container from the depicted pivoted point (O
289 in Figure 6), M_{F_D} is the torque due to the drag force (F_D), and M_{F_G} is the torque due to the effective
290 weight (F_G). Note that a uniform distribution of the contained fraction is assumed, so that the
291 downwards gravitational force direction will be coincident in a same vertical with the upwards
292 buoyancy force direction.

293 The threshold function (i.e. a relationship between flow velocity and water depth) for
294 each mode of instability has been derived also for two flow directions, parallel to L_1 and L_2 , which
295 considers different areas for drag force to act on. Therefore, four threshold functions have been
296 obtained as indicated in the expressions (13a,b) and (14a,b) given in Figure 11.

297 The two unknown parameters are the roughness coefficient (μ) and the drag coefficient
298 (C_d). Regarding the friction coefficient (μ) there exists a great uncertainty because it depends on
299 where the container is placed. In this study it is supposed to be placed on the asphalt and μ for
300 rubber against asphalt ranges from 0.25 to 0.75 according to Gerard (2006). Even so a range of
301 values may be possible so both values have been taken into account in order to define an
302 uncertainty between both functions, where the instability is possible depending on the real friction
303 coefficient value (μ).

304 According to Isyumov (2005) the drag coefficient for square cylinders with rounded
305 corners (i.e. the studied containers) may vary from 1.2 to 0.5 for a range of Reynolds numbers
306 from $1.3 \cdot 10^5$ to $2.4 \cdot 10^6$. The sensitivity of the drag coefficient (C_d) has been analysed based on
307 its effects on the stability thresholds of a lateral and 3,200 litres container, L_2 flow direction, waste
308 fraction and half-full filling scenario. In Figure 12 these thresholds have been plotted according
309 to the formulations derived, and considering the extreme values of the drag coefficient (i.e. 1.2
310 and 0.5). It can be observed that sensitivity is quite high and the importance of C_d depends on the
311 combination of the water depth and velocity that acts on the container. As expected, the higher is
312 the drag coefficient the lower is the stability threshold, especially when it comes to sliding
313 stability, though in a less sensitive manner on the toppling stability threshold. In Figure 12a, the
314 variation on the critical depths (i.e. the ones which cause the instability) for three fixed critical
315 velocities: 1, 2.5, and 4 m/s, between the minimum sliding thresholds considering both $C_d=0.5$
316 and $C_d=1.2$, has been indicated. Although the maximum difference on the critical depths is 51%
317 (i.e. 3.6 cm over 7 cm) for a velocity of 4 m/s, such high velocities are not so common and
318 velocities lower than 2.5 m/s are more likely in urban floods. Therefore, differences lower than
319 32% (i.e. 3.5 cm over 11 cm) are expected to be more likely. Moreover, a similar procedure has

320 been conducted in Figure 12b by fixing three critical depths: 10, 15, and 19 cm, and determining
321 the variability on the critical velocity. A percentage of 55% of increment on the critical velocities
322 is expected in case of employing $C_d=0.5$ instead of $C_d=1.2$. Due to the great uncertainty in this
323 coefficient, and acknowledging the need of experimental tests to accurately obtain the
324 corresponding drag coefficients for each type of container, a conservative value of $C_d=1.2$ has
325 been adopted in later applications of this study..

326 Based on the adopted coefficients and on the expressions previously described, the
327 threshold stability functions have been plotted for a lateral and 3,200 litres container, L_2 flow
328 direction, waste fraction and three filling scenarios: empty, half-full, and completely full (Figure
329 13). Two thresholds are plotted for sliding instability (i.e. Sliding min and Sliding max),
330 corresponding to the minimum expected friction coefficient ($\mu = 0.25$) and the maximum
331 expected one ($\mu = 0.75$). It is observed how the higher is the velocity the lower is the water depth
332 for the container to become unstable. For each type of container the most restrictive flow direction
333 (i.e. which offers the lower water depth values) has been selected. These thresholds are relevant
334 regardless the type of flood (i.e. stormwater, riverine or coastal) that may hit the city.

335 **4. Barcelona case study**

336 ***4.1. Barcelona hydrodynamic 1D/2D coupled model***

337 In the framework of the EU funded CORFU project (Russo *et al.* 2015), a detailed 1D/2D-
338 coupled model, which takes into account the dual drainage concept (Djordjevic *et al.*, 1999), was
339 developed using Infoworks ICM version 3.0 by Innovyze (2013). ICM solves the complete 2D
340 Saint Venant equations in a finite volume semi-implicit scheme (Godunov, 1959) with a Riemann
341 solver (Alcrudo and Mulet-Marti, 2005). Moreover, in order to achieve reliable simulations,
342 experimental expressions (Gómez *et al.*, 2011) to hydraulically characterise the inlet systems were
343 implemented.

344 Besides, an extended area was modelled in order to consider surface and sewer flows
345 coming into the Raval District, which was the Spanish case study in the CORFU project

346 (COLlaborative Research on Flood resilience in Urban areas; www.corfu7.eu), from upstream
347 catchments. The final model considered a total area of 44 km², with 3,874 nodes, 241 km of total
348 pipe length and six major storage facilities with a total capacity of 170,000 m³. A 2D mesh
349 covered the whole analysed domain with 403,822 triangles.

350 The sewer model was calibrated and validated using records of four critical rainfall events
351 that occurred in Barcelona in 2011. This data was recorded in 11 rain gages and 29 limnimeters.
352 Moreover, other data collected in the post-events emergency reports (elaborated by policemen
353 and firemen) and amateur videos recorded during the selected storm events were used to calibrate
354 surface flow (Russo *et al.*, 2015).

355 Currently, in the framework of the ongoing EU funded RESCCUE project, a more
356 extended 1D/2D model has been developed in order to study completely the entire city of
357 Barcelona, which is now the Spanish case study of the RESCCUE project. Not only a more
358 extended model has been undertaken, but also all the improvements in the drainage system since
359 2011 have been incorporated within the earlier CORFU model.

360 ***4.2. Historical real stormwater flood in Barcelona (30/07/2011)***

361 On 30th of July 2011 a heavy rainfall event occurred which caused a major flood in
362 Barcelona. The cumulative rainfall was 30.4 mm in one hour, the maximum rainfall intensity in
363 20 minutes was 105.9 mm/h (corresponding to a return period of 8 years approximately), and a
364 maximum rainfall intensity in 5 minutes was 140.4 mm/h (corresponding to a return period of 2
365 years approximately). This rainfall event was the one employed to validate the CORFU model
366 and its spatial distribution was taken into account by considering rainfall data recorded from 11
367 rain gauges across Barcelona.

368 The output of this model (i.e. water depths and velocities in each grid cell) has been
369 employed in this section in order to study the potentially unstable containers within the flooded
370 area. In this case, according to the 2D surface extent of the CORFU model, only 10,455 containers
371 out of 23,141 (45%) have been studied. In a way, the flood (i.e. CORFU model output) caused by

372 the 30th of July 2011 event has been thus employed as validation of the proposed stability criteria
373 for solid waste containers.

374 Three scenarios have been studied: containers empty, 50% filled and full, and the
375 distribution of these containers potentially unstable are shown in Figure 14.

376 In Table 4 the number of containers studied per district is shown together with the
377 percentage of them which are potentially unstable for the three scenarios. According to these
378 results, it may be stated that the most vulnerable districts in terms of potentially unstable
379 containers are Eixample and Sants-Montjuic, considering though only in this case (i.e. CORFU
380 model domain) less than a half of the total number of the containers were included in the
381 modelling.

382 A recorded video of the 30th of July 2011 flood, for a specific critical spot of Ciutat Vella
383 district is available and on it two containers are observed to be washed away (Figure 15), namely
384 a Lateral 3,200l Waste and a Lateral 2,200l Organic. According to the present containers stability
385 study, in this area one container is expected to lose its stability in case of being empty, and there
386 is a correspondence also with the volume and fraction of one of the two containers washed away
387 in reality. Therefore, this video provides a validation of the reliability of this study and, namely
388 of the adequacy of the proposed stability thresholds.

389 ***4.3. Floods related to different design storms (T= 1, 10 and 50 years)***

390 Design storms of 1, 10 and 50 years return period, 155 minutes duration, and 5 minutes
391 of time intervals have been developed by Barcelona Cicle de l'Aigua S.A. (BCASA), the public
392 company managing the sewer/stormwater system of the city, through the alternating block
393 method. The highest intensity block has been established in the minute 65, for 1 year return period,
394 and in the minute 130, for 10 and 50 years return period. These have been simulated as inputs for
395 the Barcelona hydrodynamic 1D/2D coupled model used in the framework of the ongoing EU
396 funded RESCCUE project. In this occasion, same procedure as previously described (using
397 CORFU) has been followed, although a more extended area, which covers almost the whole

398 Barcelona city, has been studied. It means 17,836 containers, out of 23,141 (77%) in Barcelona,
399 placed within the model domain and whose stability has been assessed.

400 Since 2016 fixation pieces (Figure 16a) started to be installed in order to ensure the
401 stability of containers when observed that only their own weight could cause their instability in
402 steep streets. The number of installed pieces is 147 so far, but 574 more are planned to be installed
403 in the short term. However, these pieces may be used also to ensure stability of containers located
404 in flat or low-slope areas (Figure 16b), which may be potentially unstable when an urban flood
405 occurs. Therefore, these already-fixed containers are not potentially unstable due to floodwater
406 and hence have been removed from the analysed ones.

407 In Figure 17 maps with the potentially unstable containers are shown, for the considered
408 scenarios (i.e. empty, half-full, and completely full) and return periods that caused containers'
409 instabilities (i.e. 10 and 50 years). Moreover, in Table 5 the number and percentage of containers
410 potentially unstable is shown per district. These figures indicate the most vulnerable districts to
411 be Eixample, St. Andreu, and Sants-Montjuïc. It has to be noted that some drainage network
412 improvements were carried out after the actual stormwater flood event in July 30th 2011, which
413 have been included in the complete hydrodynamic model employed in the RESCCUE project.
414 This fact, together with the installation of the previously mentioned fixation pieces for containers
415 placed on steep streets, explains the current overall flood vulnerability reduction in the city, and
416 specifically regarding containers instability.

417 ***4.4. Adaptation measures proposed***

418 Based on these findings, in order to increase the resilience of waste sector against urban
419 floods caused by a 10 years return period rainfall in Barcelona for an empty containers scenario,
420 1,668 fixation pieces would be necessary to be installed. It has to be noted that a couple of pieces
421 are needed to be installed per group of containers (Figure 16a), thus 2 pieces have been taken into
422 account per each group location where at least one potentially unstable container can be found. It
423 would mean an estimated investment of 151,788 € (91€/piece). The purpose of these pieces will

424 be to ensure the containers' stability due to floodwaters in flat areas, and due to their own weight
425 in steep streets.

426 **5. Conclusions**

427 According to the collection process for large Spanish cities (e.g. Barcelona city), before
428 the solid waste is dumped in landfills its management starts from a regular collection of household
429 waste municipal service which is carried out through street containers. When an urban flood
430 occurs those containers may lose their stability, thereby allowing debris (i.e. solid waste
431 contained) and leachate to escape from the container and contaminate floodwaters. As the waste
432 containers stability when exposed to flooding is definitely an environmental, safety and health
433 concern, this research has been focused on assessing how vulnerable against common urban flood
434 these containers are in Barcelona. Moreover, some cascading effects may be caused when
435 containers instabilities occur: traffic disruption, waste collection disruption, potential sewer
436 blockages, and increase likelihood of cascading effects due to flooding.

437 The methodology proposed here is the study of the stability of the containers when
438 exposed to urban floods, which the Barcelona City Council has distributed across the city to
439 provide waste collection to citizens. In order to do this, three main stages were carried out: 1)
440 development of a 1D/2D coupled hydrodynamic model for Barcelona city; 2) derivation of
441 stability functions for waste containers; and 3) development of a GIS map with the georeferenced
442 containers location.

443 The 1D/2D hydrodynamic model covers the entire city of Barcelona, which is the Spanish
444 case study of the RESCCUE project. The stability functions were derived based on an analysis of
445 forces acting on a flooded container by establishing equilibrium conditions for the different modes
446 of instability (i.e. sliding, toppling and floating). These functions are dependent on both hydraulic
447 variables, velocity and water depth. Moreover, the characteristics of each container (e.g. volume,
448 dimensions or fraction they may contain) will determine the shape of each function. The obtained
449 stability thresholds have been employed to analyse the potential behaviour of containers against
450 floods in Barcelona caused by historical (model validation) and design storms (i.e. 1, 10 and 50

451 years). The Barcelona City Council has performed a GIS-based map with the location of all types
452 of containers across Barcelona City. This information was essential in order to study if their
453 current location may lead to a potential instability. Therefore, the resulting outputs from the
454 hydrodynamic model (i.e. velocities and water depth within the studied domain) were related to
455 the containers and by applying the derived stability functions, those containers potentially
456 unstable have been identified. Once the containers potentially unstable are identified, adaptation
457 measures may be adopted in order to improve the resilience of waste sector against urban floods.
458 Specifically, an estimated investment in adaptation measures (i.e. installation of fixation pieces)
459 of 151,788 € would be sufficient in order to guarantee the containers stability for an empty
460 containers scenario and urban floods related to rainfalls of 10 years return period.

461 The same procedure could be followed in order to analyse the flood vulnerability for
462 containers in cities where a regular waste collection through street containers is carried out. Only
463 new and tailored stability functions according the characteristics of the containers employed in
464 the specific city should be derived, and resilient strategies such as the ones presented herein could
465 be proposed.

466 **ACKNOWLEDGMENTS**

467 The authors thank the RESCCUE project, which is funded by the EU H2020 (Grant Agreement
468 No. 700174), whose support is gratefully acknowledged.

469 **References**

- 470 Alcrudo, F. and Mulet-Marti, J. (2005). Urban inundation models based upon the Shallow Water
471 equations. Numerical and practical issues. Proceedings of Finite Volumes for Complex
472 Applications IV. Problems and Perspectives. Hermes Science Publishing. pp. 3–1. ISBN
473 1 905209 48 7.
- 474 Butler, D. and Davies, J.W. (2011). Urban drainage, third edition. Spon Press. Oxford, United
475 Kingdom. 621p.
- 476 Coaffee, J. and O’Hare, P. (2008). Urban resilience and national security: the role for planning.
477 Proc Inst Civ Eng - Urban Des Plan 161:173–182.

478 Cogersa-AstUR project (n.d.). "Caracterización de los residuos domésticos mezclados de
479 Asturias" (Mixed domestic waste characterization in Asturias (Spain)). Online:
480 <http://www.cogersa.es/metaspaces/portal/14498/50093>

481 DifferenceBetween.Com (2011). "Difference Between Density and Bulk Density". Published on
482 July 30, 2011. Online: [http://www.differencebetween.com/difference-between-density-](http://www.differencebetween.com/difference-between-density-and-vs-bulk-density/)
483 [and-vs-bulk-density/](http://www.differencebetween.com/difference-between-density-and-vs-bulk-density/)

484 Djordjevic, S., Prodnovic, D. and Maksimovic, C. (1999). An approach to simulation of dual
485 drainage. *Water Sci Technol* 39:95–103.

486 Escarameia, M. (2016). Improving urban resilience to flooding: a vital role for civil engineers.
487 *Proc Inst Civ Eng - Civ Eng* 169:101–101.

488 Evans, B., Chen, A., Prior, A., Djordjević, S., Savic, D., Butler, D., Goodey, P., Stevens, J.R. and
489 Colclough, G. (2018). Mapping urban infrastructure interdependencies and fuzzy risks.
490 *Procedia Engineering*. 212: 816-823.

491 Gerard, M. (2006). Tire-road friction estimation using slip-based observers. Master Thesis.
492 Department of Automatic Control, Lund University, Sweden.

493 Godunov, S.K. (1959). A difference scheme for numerical solution of discontinuous solution of
494 hydrodynamic equations. *Math. Sbornik*, 47, 271–306, translated US Joint Publ. Res.
495 Service, JPRS 7226.

496 Gómez, M. and Russo, B. (2011). Methodology to estimate hydraulic efficiency of drain inlets.
497 *Proceedings of the ICE – Water Management Institution of Civil Engineers*, 164, (1), 1–
498 10.

499 Innovyze. InfoWorks ICM (Integrated Catchment Modeling) v.2.5. (2013). User manual
500 references.

501 Isyumov, N. (2015). Wind Engineering Terminology. 14th International Conference of Wind
502 Engineering (ICWE-14). Porto Alegre, Brazil. 18p.

503 Lamond, J., Bhattacharya, N. and Bloch, R. (2012). The role of solid waste management as a
504 response to urban flood risk in developing countries, a case study analysis. In: Proverbs,
505 D., Mambretti, S., Brebbia, C. and de Wrachien, D., eds. *Flood Recovery Innovation and*
506 *Response*. (3) Southampton: WIT Press, pp. 193-205.

507 Lhomme, S., Serre, D., Diab, Y. and Laganier, R. (2013). Analyzing resilience of urban networks:
508 a preliminary step towards more flood resilient cities. *Nat Hazards Earth Syst Sci* 13:221–
509 230.

510 Martínez-Gomariz E. (2016). Inundaciones Urbanas: Criterios de Peligrosidad y Evaluación del
511 Riesgo para Peatones y Vehículos (Urban floods: Hazard Criteria and Risk assessment
512 for pedestrians and vehicles). PhD Thesis, Technical University of Catalonia. Barcelona,
513 Spain, 566 p.

514 Martínez-Gomariz, E., Gómez, M., Russo, B. (2016). Experimental study of the stability of
515 pedestrians exposed to urban pluvial flooding. *Natural Hazards*. 82:1259–1278.

516 Martínez-Gomariz, E., Gómez, M., Russo, B., Djordjević, S. (2018). Stability criteria for flooded
517 vehicles: a state-of-the-art review. *Journal of Flood Risk Management*. 10: 817-826.

518 Martínez-Gomariz, E., Gómez, M., Russo, B., Djordjević, S. (2017). A new experiments-based
519 methodology to define the stability threshold for any vehicle exposed to flooding. *Urban
520 Water Journal*, 14:930–939.

521 Meerow, S, Newell, JP, Stults, M. (2016) Defining urban
resilience: A review. *Landsc Urban Plan* 147:38–49.

522 Nanía, L.S., León, A.S. and García, M.H. (2015). Hydrologic-Hydraulic Model for Simulating
523 Dual Drainage and Flooding in Urban Areas: Application to a Catchment in the
524 Metropolitan Area of Chicago. *J Hydrol Eng* 20:4014071.

525 Patra, J. P., Kumar, R. and Mani, P. (2016). Combined fluvial and pluvial flood inundation
526 modelling for a project site. *Procedia Technology*. 24, 93-100.

527 Russo, B., Sunyer, D., Velasco, M. and Djordjević, S. (2015). Analysis of extreme flooding events
528 through a calibrated 1D/2D coupled model: the case of Barcelona (Spain). *Journal of
529 Hydroinformatics*. 473-491.

530 Russo, B., Velasco, M. and Suñer, D. (2013). Flood hazard assessment considering climate
531 change impacts-Application to Barcelona case study using a 1D/2D detailed coupled
532 model. In: *International Conference on Flood Resilience: Experiences in Asia and
533 Europe*. Exeter, United Kingdom, 10p.

534 Sam, P.A., (2002). *Are the Municipal Solid Waste Management Practices Causing Flooding
535 During the Rainy Season in Accra, Ghana, West Africa*. University of Kansas, AERCG
536 Department Of Geography/Environmental Studies. Lawrence, KS, USA, 17p.

537 Schmitt, T.G., Thomas, M., Ettrich, N. (2004). Analysis and modeling of flooding in urban
538 drainage systems. *J Hydrol* 299:300–311.

539 The Spanish Ministry of Agriculture and Fisheries, Food and Environment (MAPAMA) (n.d.).
540 “Biorresiduos. ¿Qué características tienen?” (Biowaste. What are their characteristics?).
541 online: <http://www.mapama.gob.es/es/calidad-y-evaluacion-ambiental/temas/prevencion-y-gestion-residuos/flujos/biorresiduos/Biorresiduos-Que-caracteristicas-tienen.aspx>

542
543

544 UN-HABITAT (2010). *Solid waste management in the world’s cities*. Earthscan. London, United
545 Kingdom. 228p.

546 United States Agency for International Development (USAID) (2012). *Addressing climate
547 change impacts on infrastructure. Preparing for change*. Technical Report. 52p. Global
548 Climate Change Office, Climate Change Resilient Development project. Washington,

549 DC. USA. (Online: <http://www.ccrdproject.com/ccrd-library/infrastructure>, accessed
550 4/05/2017)

551 United States Agency for International Development (USAID) (2014). Climate-Resilient
552 Development: A Framework for Understanding and Addressing Climate Change.
553 Technical Report. Global Climate Change Office, Climate Change Resilient
554 Development project. Washington, DC. USA. 40p. (Online:
555 <http://www.usaid.gov/climate/climate-resilient-development-framework>, accessed
556 4/05/2017)

557 United States Agency for International Development (USAID) (2015). Climate resilient
558 Infrastructure services: lessons learned. Technical Report. 36p. Global Climate Change
559 Office, Climate Change Resilient Development project. Technical report. Washington,
560 DC. USA. (Online: <http://www.ccrdproject.com/ccrd-library/cris>).

561 Winne, S., Horrocks, L., Kent, N., Miller, K., Hoy, C., Benzie, M. and Power, R. (2012).
562 Increasing the climate resilience of waste infrastructure. Final Report under Defra
563 contract ERG 1102. AEA group, published by Defra.

564 Kundzewicz, Z. W., Kanae, S., Seneviratne, S. I., Handmer, J., Nicholls, N., Peduzzi, P., Mechler,
565 R., Bouwer, L.M., Arnell, N., Mach, K., Muir-Wood, R., Brakenridge, G.R., Kron, W.,
566 Benito, G., Honda, Y., Takahashi, K. and Sherstyukov, B. (2014). Flood risk and climate
567 change: global and regional perspectives. *Hydrological Sciences Journal*, 59(1), 1-28.

568 Zevenbergen, C., Cashman, A., Evelpidou, N., Pasche, E., Garvin, S., and Ashley, R. (2010).
569 Urban Flood Management, CRC Press, first edition, 340 pp.

570 Zimmerman, R. and Faris, C. (2010). "Chapter 4: Infrastructure Impacts and Adaptation
571 Challenges." In New York City Panel on Climate Change 2010 Report. *Annals of the*
572 *New York Academy of Sciences*, 1196: 63–86.
573

574



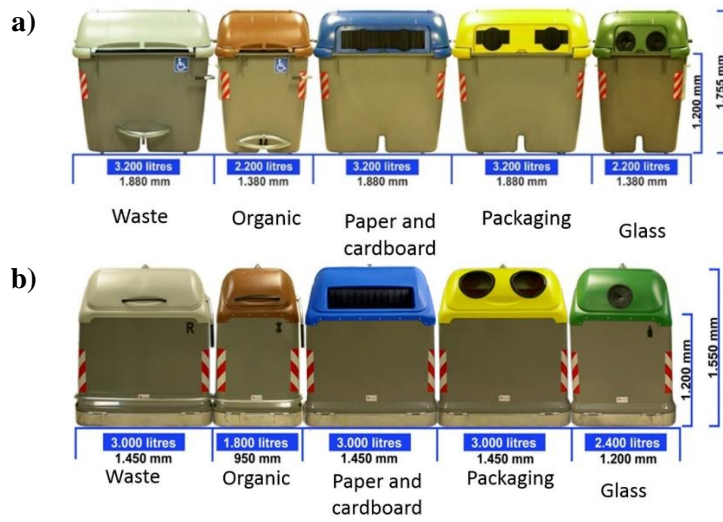
575



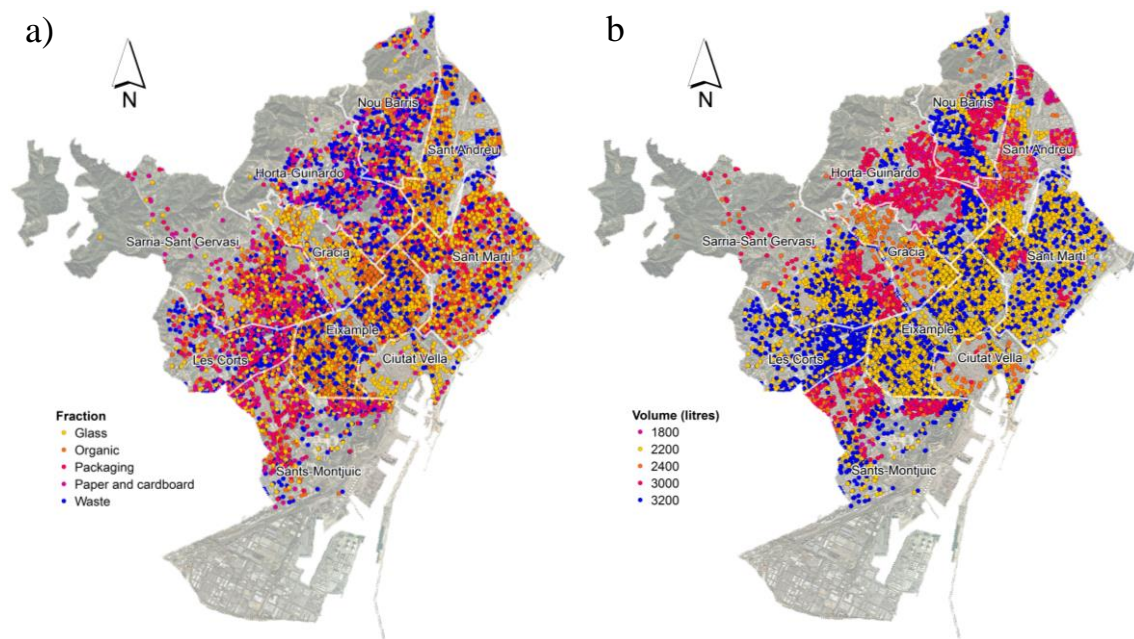
576

Figure 1: Real containers removed due to flooding in Barcelona

577



578 Figure 2: Types of containers in Barcelona: a) lateral load, and b) bilateral load
579



580

581 **Note:** due to the great amount of containers, in some cases a dot indicates a location for a set of even five
 582 containers of different fractions/volumes. Therefore, within the map only a type of container, either
 583 classified by volume or fraction, is represented for each dot.

584 Figure 3: Containers distribution in Barcelona classified according to a) Fraction type, and b)

585 Volume

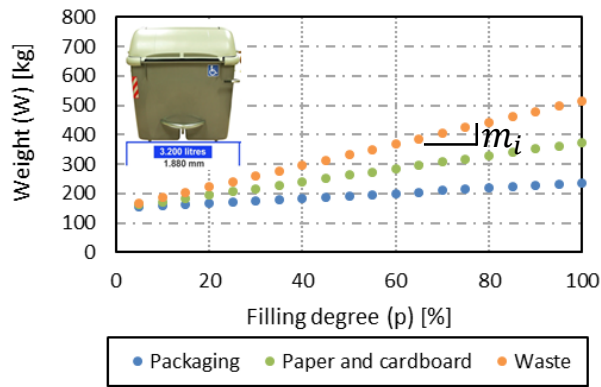
586



587

588 Figure 4: Positioning of the containers on the street

589

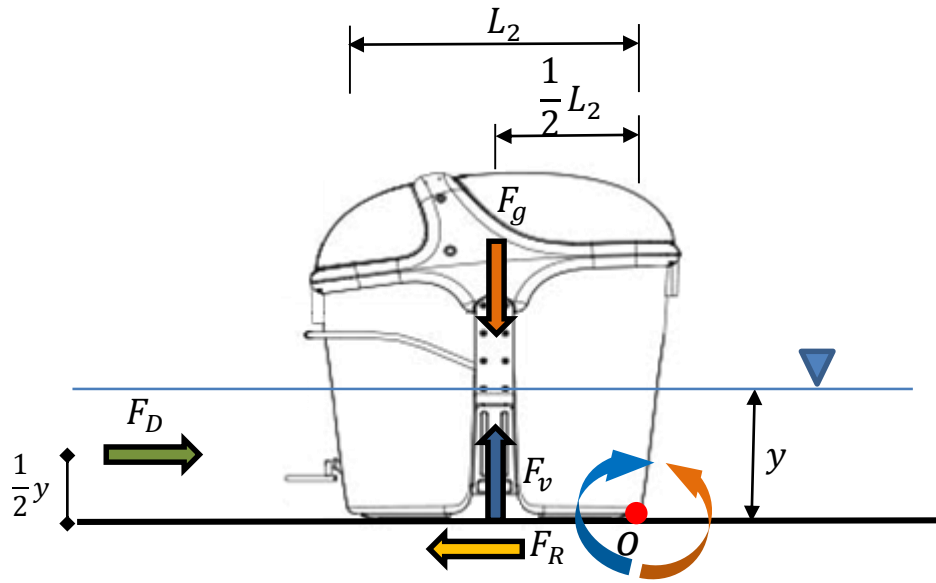


590

591 Figure 5: Container's weight functions for a volume of 3,200l and three different fraction types

592 (Packaging, paper and cardboard, and waste) according to its filling degree (p (%))

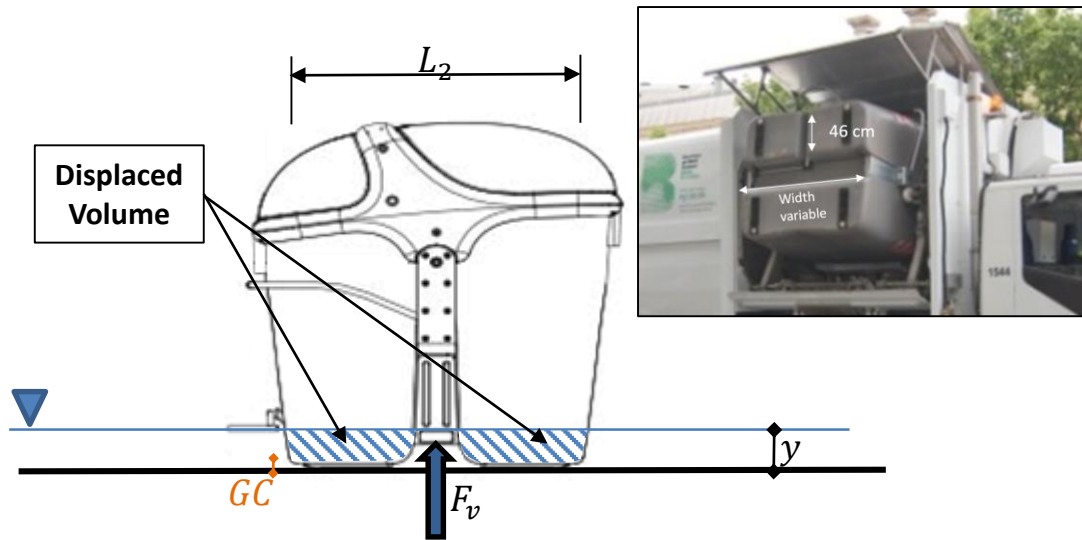
593



594

595 Figure 6: Forces acting on a flooded container (Flow direction parallel to L_2)

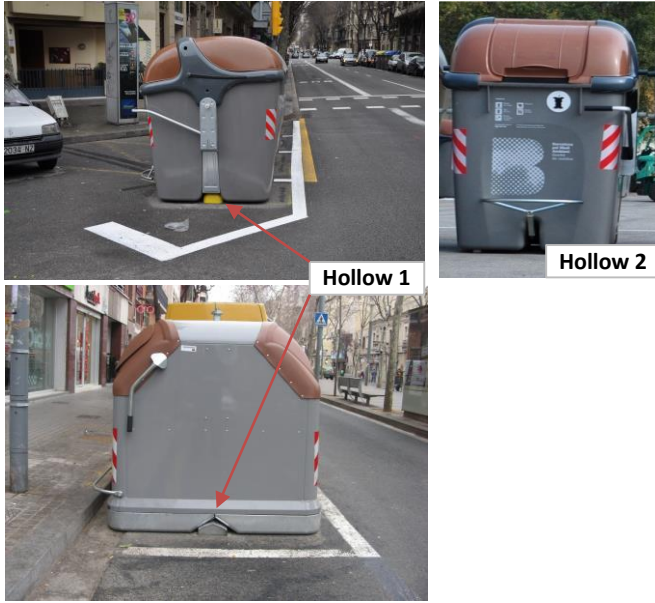
596



597

598 Figure 7: Displaced volume in a flooded container

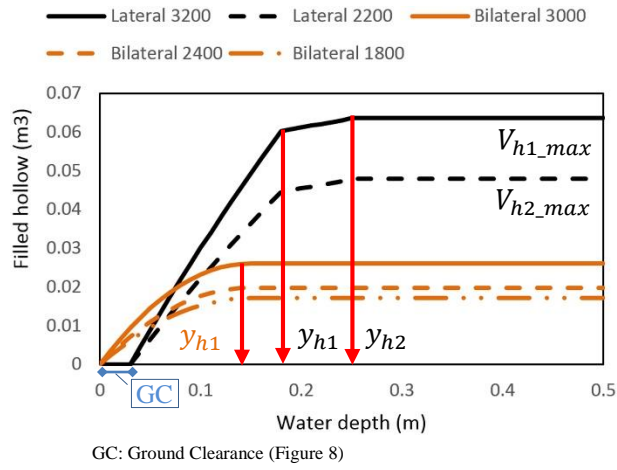
599



600

601 Figure 8: Hollows in the containers' base

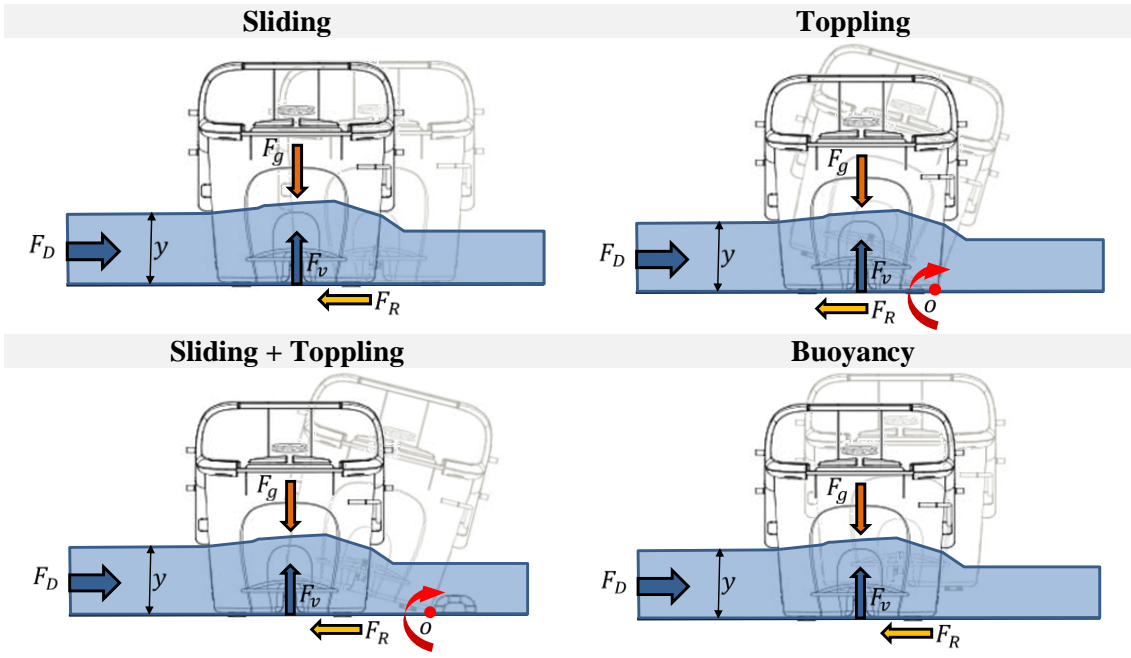
602



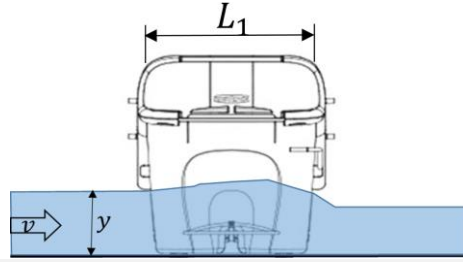
603
604

605 Figure 9: Water filling hollows functions ($V_h(y)$)

606



607 Figure 10: Different modes of instability for a flooded container
 608



Sliding

$$(v_s)^{L1} = \sqrt{\frac{2 \cdot \mu \cdot [g(W_0 + m_i \cdot P / 100) - \gamma_w \cdot (L_1 \cdot L_2 \cdot (y - GC) - V_H(y))]}{\rho_w \cdot C_d \cdot (y - GC) \cdot L_2}} \quad (13a)$$

Toppling

$$(v_t)^{L1} = \sqrt{\frac{2 \cdot L_1 \cdot [g(W_0 + m_i \cdot P / 100) - \gamma_w \cdot (L_1 \cdot L_2 \cdot (y - GC) - V_H(y))]}{\rho_w \cdot C_d \cdot (y - GC) \cdot y \cdot L_2}} \quad (14a)$$

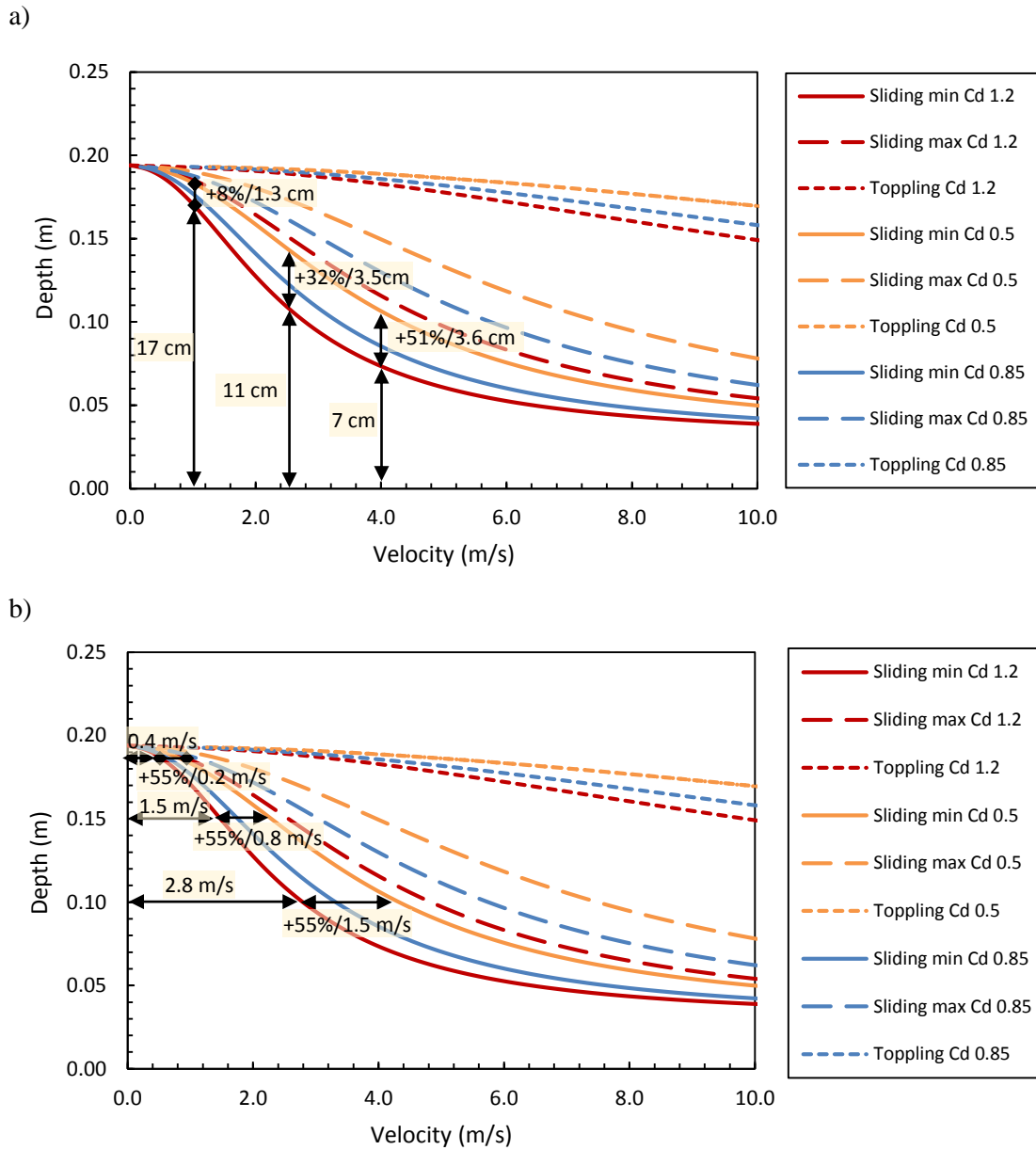
Sliding

$$(v_s)^{L2} = \sqrt{\frac{2 \cdot \mu \cdot [g(W_0 + m_i \cdot P / 100) - \gamma_w \cdot (L_1 \cdot L_2 \cdot (y - GC) - V_H(y))]}{\rho_w \cdot C_d \cdot (y - GC) \cdot L_1}} \quad (13b)$$

Toppling

$$(v_t)^{L2} = \sqrt{\frac{2 \cdot L_2 \cdot [g(W_0 + m_i \cdot P / 100) - \gamma_w \cdot (L_1 \cdot L_2 \cdot (y - GC) - V_H(y))]}{\rho_w \cdot C_d \cdot (y - GC) \cdot y \cdot L_1}} \quad (14b)$$

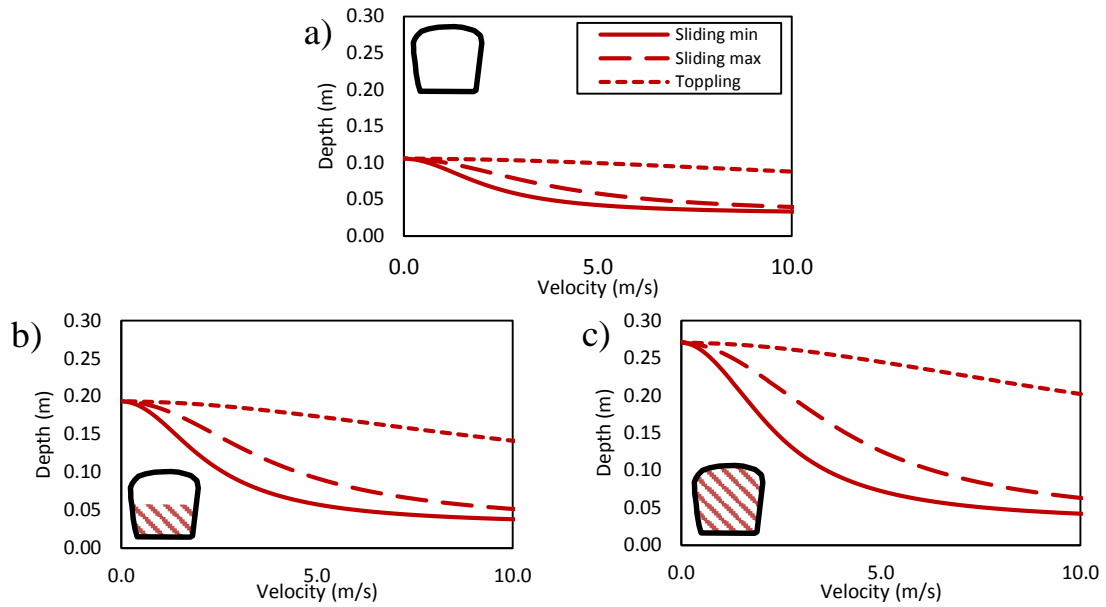
609 Figure 11: Threshold functions for sliding and toppling instabilities according to two flow
 610 directions (L1 or L2)
 611



612 Figure 12. Drag coefficient sensitivity on the sliding and toppling stability thresholds (min:
 613 $\mu=0.25$ and max: $\mu=0.75$) for a lateral and 3,200 l container, L2 flow direction, waste fraction
 614 and 50% filled container scenario.

615

616



617 Figure 13. Sliding and toppling stability thresholds ($C_d=1.2$, $\mu_{\min}=0.25$, and $\mu_{\max}=0.75$) for a
 618 lateral and 3,200 l container, L2 flow direction, waste fraction and a) empty container scenario,
 619 b) 50% filled container scenario, and c) full container scenario

620

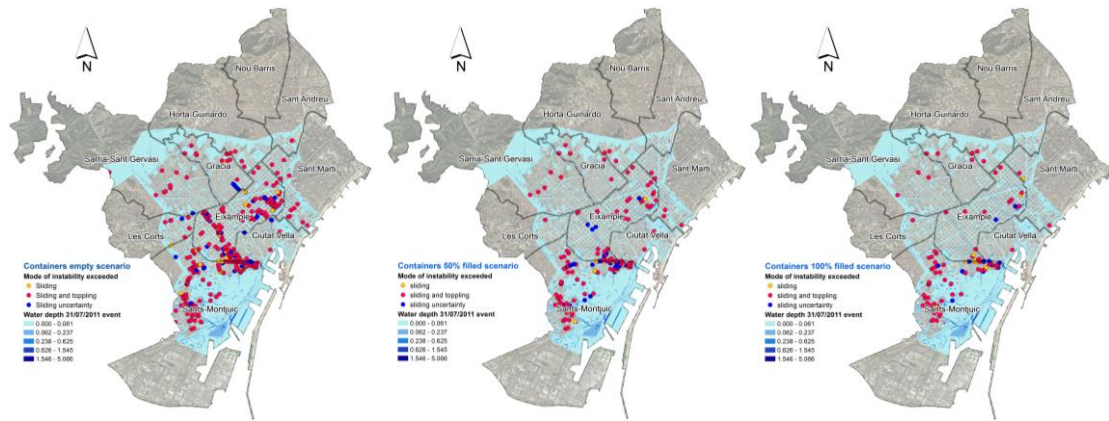
621

622

623

624

625



626

627 Figure 14: Potentially unstable containers due to sliding and/or toppling in Barcelona for the
 628 three considered scenarios (containers empty, 50% filled and full) according to 30/07/2011
 629 event.
 630



631
632
633

Note: Only the empty containers scenario offers instabilities.

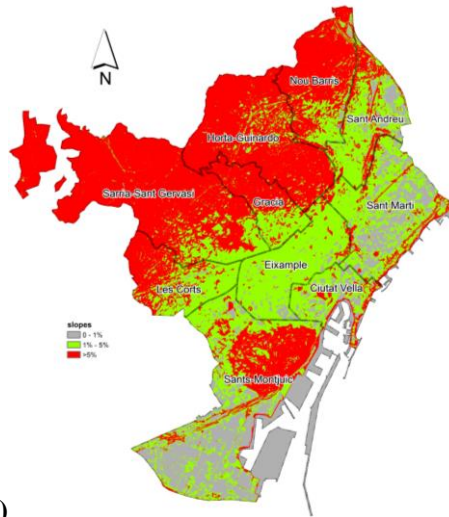
634
635
636

Figure 15: Validation of the present containers stability study based on a recorded video of the 30th of July 2011 flood in Ciutat Vella district.

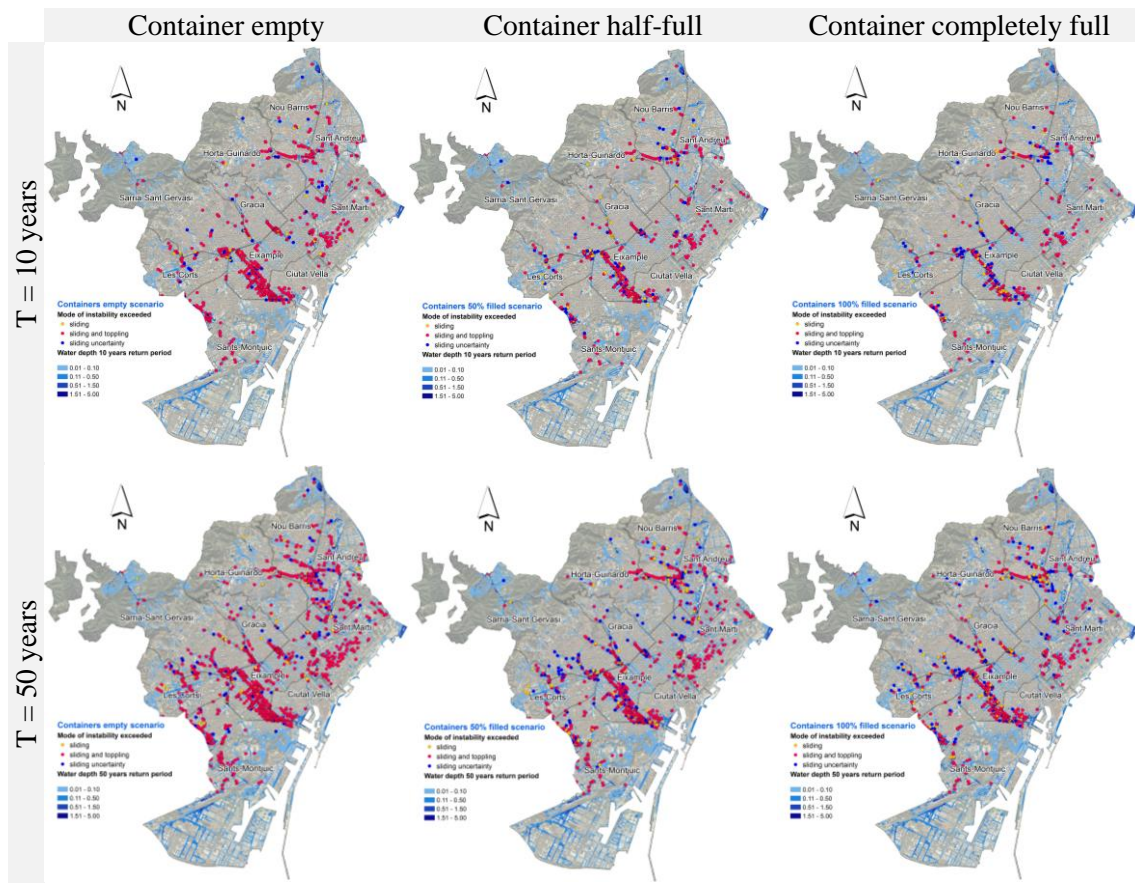
a)



b)



637 Figure 16: a) Fixation piece example, currently installed in 147 locations within Barcelona city,
638 and b) slopes map of Barcelona city.
639



640 Figure 17: Potentially unstable containers due to sliding and/or toppling in Barcelona for the
 641 three considered scenarios (containers empty, 50% filled and full) according to 10 and 50 years
 642 return period design storms.
 643

644 Table 1. Total number of containers in Barcelona and studied ones per districts and type of
 645 fraction

District	# of containers	Total # of studied containers	Distribution of studied containers per fraction					% studied
			Waste	Organic	Paper and cardboard	Packaging	Glass	
Ciutat Vella	1,147	624	152	74	134	130	134	54
Eixample	4,864	4,808	2,213	1,153	477	485	481	99
Sants-Montjuic	2,976	2,369	952	487	313	310	307	80
Les Corts	1,648	1,602	740	218	195	194	192	97
Sarrià-St. Gervasi	3,843	2,528	1,107	472	325	315	309	66
Gràcia	2,135	1,246	394	275	196	188	193	58
Horta-Guinardó	2,463	2,194	730	472	330	332	330	89
Nou Barris	2,144	1,941	661	391	298	294	297	90
St. Andreu	1,986	1,901	713	384	268	268	268	96
St. Martí	3,928	3,928	1,483	831	540	542	532	100

646
 647
 648
 649




650 Table 2. Characteristics of different types of containers in Barcelona

Load	Volume (l)	Fraction	Units (u)	GC [m]	L ₁ [m]	L ₂ [m]	V _{hollow1} (m ³)	V _{hollow2} (m ³)	Unladen weight (kg)	m _i (kg)
Lateral	3,200	Packaging	2,044	0.03	1.70	1.45	0.054	0.015	150	0.85
Lateral	3,200	Paper and cardboard	2,041	0.03	1.70	1.45	0.054	0.015	150	2.24
Lateral	3,200	Waste	7,033	0.03	1.70	1.45	0.054	0.015	150	3.65
Lateral	2,200	Organic	3,684	0.03	1.20	1.45	0.038	0.015	120	8.53
Lateral	2,200	Glass	2,034	0.03	1.20	1.45	0.038	0.015	120	7.26
Bilateral	3,000	Packaging	1,013	0	1.45	1.60	0.026	-	295	0.80
Bilateral	3,000	Paper and cardboard	1,035	0	1.45	1.60	0.026	-	295	2.10
Bilateral	3,000	Waste	2,112	0	1.45	1.60	0.026	-	295	3.42
Bilateral	1,800	Organic	1,136	0	0.95	1.60	0.017	-	195	6.98
Bilateral	2,400	Glass	1,009	0	1.10	1.60	0.022	-	250	7.92

651

652

653 Table 3. Critical depths for the different containers and according to three scenarios: empty,
 654 50% filled and full.

Type of Container			Picture	Critical depth (m) according to filling (%)		
Loading	Volume	Fraction		0%	50%	100%
Lateral	3,200	Packaging		0.106	0.127	0.148
		Paper and cardboard		0.106	0.162	0.212
		Waste		0.106	0.194	0.271
	2,200	Organic		0.118	0.386	0.640
		Glass		0.118	0.349	0.565
	Bilateral	3,000	Packaging		0.139	0.156
Paper and cardboard				0.139	0.184	0.229
Waste				0.139	0.213	0.286
2,400		Glass		0.155	0.380	0.605
1,800		Organic		0.146	0.369	0.599

655
 656

657 Table 4. Number of flooded containers within the CORFU model domain per districts and
 658 percentage of containers potentially unstable.

District	# of containers	Total # of studied containers	Total # of flooded containers within the CORFU domain	Containers potentially unstable according to considered scenarios		
				Empty	Half-full	Completely full
Ciutat Vella	1,147	624	420	18 (4.3%)	5 (1.2%)	3 (0.7%)
Eixample	4,864	4,808	2,822	281 (10.0%)	73 (2.6%)	37 (1.3%)
Sants-Montjuic	2,976	2,369	1,722	503 (29.2%)	248 (14.4%)	143 (8.3%)
Les Corts	1,648	1,602	682	15 (2.2%)	2 (0.3%)	1 (0.1%)
Sarrià-St. Gervasi	3,843	2,528	2,014	25 (1.2%)	8 (0.4%)	6 (0.3%)
Gràcia	2,135	1,246	685	41 (6.0%)	9 (1.3%)	5 (0.7%)
Horta-Guinardó	2,463	2,194	728	14 (1.9%)	9 (1.2%)	9 (1.2%)
Nou Barris	2,144	1,941	0	-	-	-
St. Andreu	1,986	1,901	244	2 (0.8%)	0 (0.0%)	0 (0.0%)
St. Martí	3,928	3,928	1,138	32 (2.8%)	10 (0.9%)	5 (0.4%)

659
 660
 661

662 Table 5. Number of flooded containers within the RESCCUE model domain per districts and
 663 percentage of containers potentially unstable.

District	Containers			Containers potentially unstable (# (%)) according to considered scenarios								
	Units	Units studied	Units flooded within the RESCCUE domain	T = 1 years			T = 10 years			T = 50 years		
				0%	50%	100%	0%	50%	100%	0%	50%	100%
Ciutat Vella	1,147	624	460	0 (0.00%)	0 (0.00%)	0 (0.00%)	80 (17.4%)	65 (14.1%)	59 (12.8%)	92 (20.0%)	82 (17.8%)	74 (16.1%)
Eixample	4,864	4,808	2,845	0 (0.00%)	0 (0.00%)	0 (0.00%)	477 (16.8%)	301 (10.6%)	218 (7.7%)	702 (24.7%)	462 (16.2%)	343 (12.1%)
Sants-Montjuic	2,976	2,369	2,107	0 (0.00%)	0 (0.00%)	0 (0.00%)	230 (10.9%)	138 (6.5%)	96 (4.6%)	481 (22.8%)	315 (15.0%)	232 (11.0%)
Les Corts	1,648	1,602	1,499	0 (0.00%)	0 (0.00%)	0 (0.00%)	141 (9.4%)	63 (4.2%)	40 (2.7%)	224 (14.9%)	141 (9.4%)	94 (6.3%)
Sarrià-St. Gervasi	3,843	2,528	2,348	0 (0.00%)	0 (0.00%)	0 (0.00%)	170 (7.2%)	96 (4.1%)	72 (3.1%)	313 (13.3%)	208 (8.9%)	158 (6.7%)
Gràcia	2,135	1,246	801	0 (0.00%)	0 (0.00%)	0 (0.00%)	34 (4.2%)	30 (3.7%)	29 (3.6%)	58 (7.2%)	41 (5.1%)	36 (4.5%)
Horta-Guinardó	2,463	2,194	1,782	0 (0.00%)	0 (0.00%)	0 (0.00%)	67 (3.8%)	48 (2.7%)	42 (2.4%)	98 (5.5%)	70 (3.9%)	62 (3.5%)
Nou Barris	2,144	1,941	1,788	0 (0.00%)	0 (0.00%)	0 (0.00%)	150 (8.4%)	109 (6.1%)	92 (5.1%)	239 (13.4%)	179 (10.0%)	152 (8.5%)
St. Andreu	1,986	1,901	1,270	0 (0.00%)	0 (0.00%)	0 (0.00%)	171 (13.5%)	94 (7.4%)	66 (5.2%)	319 (25.1%)	189 (14.9%)	131 (10.3%)
St. Martí	3,928	3,928	2,936	0 (0.00%)	0 (0.00%)	0 (0.00%)	264 (9.0%)	151 (5.1%)	98 (3.3%)	555 (18.9%)	285 (9.7%)	193 (6.6%)

664